Front. Environ. Sci. Eng. 2021, 15(4): 75
https://doi.org/10.1007/s11783-020-1368-0

RESEARCH ARTICLE

# Mechanisms for simultaneous ozonation of sulfamethoxazole and natural organic matters in secondary effluent from sewage treatment plant

**Xinshu Liu, Xiaoman Su, Sijie Tian, Yue Li, Rongfang Yuan (✉)**

Beijing Key Laboratory of Resource-oriented Treatment of Industrial Pollutants, Department of Environmental Science and Engineering, University of Science and Technology Beijing, Beijing 100083, China

## HIGHLIGHTS

- SMX was mainly degraded by hydrolysis, isoxazole oxidation and double-bond addition.
- Isoxazole oxidation and bond addition products were formed by direct ozonation.
- Hydroxylated products were produced by indirect oxidation.
- NOM mainly affected the degradation of SMX by consuming $^{\bullet}OH$ rather than $O_3$.
- Inhibitory effect of NOM on SMX removal was related to the components' aromaticity.

## GRAPHIC ABSTRACT

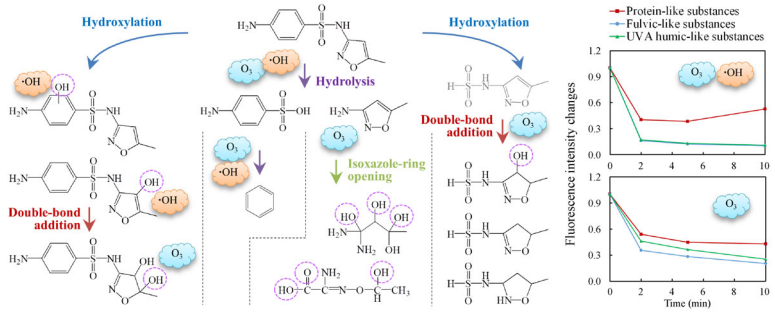


## ARTICLE INFO

*Article history:*
Received 29 June 2020
Revised 29 September 2020
Accepted 5 October 2020
Available online 16 November 2020

*Keywords:*
Sulfamethoxazole
Ozonation
Natural organic matters
Secondary effluent
Degradation mechanism

## ABSTRACT

Sulfamethoxazole (SMX) is commonly detected in wastewater and cannot be completely decomposed during conventional treatment processes. Ozone ($O_3$) is often used in water treatment. This study explored the influence of natural organic matters (NOM) in secondary effluent of a sewage treatment plant on the ozonation pathways of SMX. The changes in NOM components during ozonation were also analyzed. SMX was primarily degraded by hydrolysis, isoxazole-ring opening, and double-bond addition, whereas hydroxylation was not the principal route given the low maximum abundances of the hydroxylated products, with *m/z* of 269 and 287. The hydroxylation process occurred mainly through indirect oxidation because the maximum abundances of the products reduced by about 70% after the radical quencher was added, whereas isoxazole-ring opening and double-bond addition processes mainly depended on direct oxidation, which was unaffected by the quencher. NOM mainly affected the degradation of micropollutants by consuming $^{\bullet}OH$ rather than $O_3$ molecules, resulting in the 63%–85% decrease in indirect oxidation products. The NOM in the effluent were also degraded simultaneously during ozonation, and the components with larger aromaticity were more likely degraded through direct oxidation. The dependences of the three main components of NOM in the effluent on indirect oxidation followed the sequence: humic-like substances>fluvic-like substances>protein-like substances. This study reveals the ozonation mechanism of SMX in secondary effluent and provides a theoretical basis for the control of SMX and its degradation products in actual water treatment.



## 1 Introduction

The water pollution caused by antibiotics has aroused global concerns given the extensive production and consumption of antibiotics, resulting in hazards to the aquatic environment and human health (Yuan et al., 2019; Li et al., 2020a). A sulfonamide antibiotic, sulfamethoxazole (SMX) is commonly detected in municipal wastewater (Wang and Zhuan, 2020), with concentration reaching 0.1–1.9 μg/L in wastewater effluents (Kong et al., 2020); its concentration in hospital wastewater is 4–150 times higher than that in domestic wastewater

✉ Corresponding author
E-mail: yuanrongfang@ustb.edu.cn

(Khan et al., 2020c). SMX can be partially removed in conventional treatment plants (Trovó et al., 2009; Hai et al., 2020; Milh et al., 2020). Therefore, the treatment of these micropollutants need special attention and target removal (Khan et al., 2020b; Li et al., 2020b).

As one of the substances with the strongest oxidizability in nature, ozone ($O_3$) is often used during water treatment (Ye et al., 2019; Zhao et al., 2019; Graça et al., 2020; Mao et al., 2020), and it has been demonstrated to oxidize antibiotics (Khan et al., 2020a). $O_3$ can react quickly with organics containing electron-rich functional groups, including olefins (such as aromatic C = C bonds), phenols, and anilines (Wang et al., 2019). Furthermore, $O_3$ may be decomposed to produce hydroxyl radicals ($^{\bullet}OH$) that can non-selectively oxidize most organic compounds with second-order rate constants as high as $10^8$–$10^9$ L/mol/s (Buxton et al., 1988; Chen et al., 2019); however, most C = C double- and C ≡ C triple-bonds cleave more rapidly than C – C or C – H bonds (Westerhoff et al., 1999). SMX can be oxidized effectively through ozonation (Willach et al., 2017; Ninwiwek et al., 2019; Ioannidi et al., 2020), resulting in its hydroxylation, fracture, and other oxidation pathways (Gçmez-Ramos et al., 2011). The aniline moiety of SMX is the main reactive site during ozonation, whether in experiments (Willach et al., 2017) or computations (Zhang et al., 2017b).

Several natural organic matters (NOM) exist in secondary effluent of sewage treatment plants. The presence of these NOM may affect the ozonation of SMX given that they can react with $O_3$ or $^{\bullet}OH$, resulting in the reduction of SMX removal rate (Lee and Lee, 2007). However, NOM can trigger the generation of $^{\bullet}OH$ radical (Ho et al., 2002). To date, studies mainly focus on the influence of NOM on the removal rates of antibiotics but rarely on the decomposition pathways of pollutants (Wang and Chu, 2016). NOM in water may exhibit different effects on different degradation pathways of the same antibiotics. For a photocatalytic process that is based on the oxidation effect of activated radicals, the products of ciprofloxacin generated from hydroxylation and defluorination are generally suppressed by NOM, whereas dealkylated and piperazine ring oxidation products are promoted (Li and Hu, 2018); in SMX photocatalytic oxidation, hydroxylation and isoxazole ring oxidation are inhibited by NOM, and most of the hydrolysis products are favored in its presence (Yuan et al., 2019). However, for the ozonation process related to both direct and indirect oxidations, the effects of NOM on antibiotic decomposition pathways remain unclear, whereas their effects on direct oxidation by $O_3$ molecules and indirect oxidation by $^{\bullet}OH$ lack proper distinction.

NOM in water can also be degraded during ozonation (Graça et al., 2020; Zhang et al., 2020). Three-dimensional excited emission matrix fluorescence spectroscopy (3DEEMFS) is considered a powerful tool for characterizing NOM in aquatic organisms (Yu et al., 2019; Xiao et al., 2020) because it can detect specific fluorescent components in NOM with high sensitivity (Coble, 1996) and without destroying the structure of components during analysis (Zhou et al., 2013).

The ozonation mechanism of SMX in actual water may differ from that in ultrapure water. However, the influence mechanism of NOM on SMX ozonation pathways is unclear. This study aimed to explore the effect of NOM on the ozonation of SMX in actual water. The normalized abundances of the ozonation products of SMX in ultrapure water and secondary effluent were detected to explore the influence of NOM on SMX degradation pathways. The direct oxidation pathways of SMX by $O_3$ molecules were obtained by adding *tert*-butanol (*t*-BuOH) as the $^{\bullet}OH$ quencher (Willach et al., 2017) to the SMX solution. In addition, 3DEEMFS analysis was employed to examine the changes in NOM components during the ozonation process, and the relationship between the properties of NOM components and their degradation mechanism was revealed. This study can provide a theoretical basis for the control of SMX and its degradation products during actual water treatment.

## 2 Materials and methods

### 2.1 Reagents

SMX (⩾98%), *t*-BuOH (⩾99.8), and formic acid (⩾98%) were purchased from Sigma-Aldrich (USA). Chromatographic-grade methanol was obtained from J.T. Baker (USA). Analytically pure sodium thiosulfate ($Na_2S_2O_8$), potassium iodide (KI), hydrochloric acid (HCl), and sodium hydroxide (NaOH) were obtained from Sinopharm Chemical Reagent Co., Ltd (China). Ultrapure water was produced by a Milli-Q system (Synergy 185, Merck Millipore, USA).

The secondary effluent was provided by a sewage treatment plant in Beijing, China. The water parameters were as follows: chemical oxidation demand (COD): 37 mg/L; total nitrogen: 22 mg/L; total phosphorus: 0.3 mg/L; pH: 7.6. The pH of the ultrapure water and secondary effluent was adjusted to 6.0 before they were used.

### 2.2 Ozonation experiments

#### 2.2.1 Ozonation in $O_3$ solution

In this study, $O_3$ gas, which was produced by an $O_3$ gas generator (3S-Λ3, Beijing Tonglin Technology Co., Ltd, China) equipped with an oxygenator (FY5W, Beijing Beichen Yaao Technology Co., Ltd, China), was introduced to a 250 mL beaker containing 100 mL ultrapure water in ice bath. Samples were obtained after a certain time to determine the $O_3$ concentration using “Standard

Methods for the Examination of Water and Wastewater (21st Ed) - APHA (2005) - Method 4500-$O_3$ - Indigo Colorimetric Method" (Bader and Hoigné, 1981). The SMX stock solution (20 mg/L) was injected into the $O_3$ solution, and the initial SMX concentration was adjusted to 200 µg/L. The samples were retrieved at 1 min after the addition of the SMX solution. Then, the effect of the initial $O_3$ concentration on the removal rate of 10 mg/L SMX was investigated.

To study the direct ozonation of SMX, 150 mmol/L *t*-BuOH was added to quench the •OH radical, and the removal rate of SMX was compared with that in the absence of *t*-BuOH. Experiments on the secondary effluent were conducted, and the experimental method was similar to that used for ultrapure water, except that actual water with a COD of 19 mg/L (diluted by $O_3$ solution) was used. All the experiments were carried out in triplicate.

#### 2.2.2 Ozonation in $O_3$ contactor

To investigate the ozonation pathways of SMX, experiments were conducted in the $O_3$ contactor containing 10 mg/L SMX solution with an initial pH of approximately 6.0. The $O_3$ gas was aerated continuously at 20°C. The reactor was stirred with a magnetic stirrer, and the excess $O_3$ was absorbed by KI solution (Fig. S1). Samples (1 mL) were obtained at regular intervals, and their reaction was terminated by adding 0.5 mL 1.0 g/L $Na_2S_2O_8$ solution.

### 2.3 Analytical methods

The SMX concentrations and the abundances of intermediate products during ozonation were determined by a high-performance liquid chromatography-tandem mass spectrometry system (Agilent 1290-6460, USA) equipped with an Agilent C18 column (3.5 µm, 2.1 mm × 150 mm). Text S1 in the Supplementary Material presents the related methods.

Fluorescence spectrometer (FS5, Edinburgh Instruments, UK) was used to measure the changes in the fluorescence of substances during the reaction. The parameters were set as follows: scanning speed: 12000 nm/min; data interval: 5.0 nm; excitation and emission light bandwidths: 3.0 nm. The excitation ($E_x$) and emission wavelengths ($E_m$) were set to 230–450 and 260–550 nm, respectively.

## 3 Results and discussion

### 3.1 Removal rates

The ozonation of SMX followed the second-order rate kinetics, and the removal rate of SMX at 1 min was detected. The effect of $O_3$ dosage on the removal rates of SMX in different conditions was investigated, and the results are shown in Fig. 1.

#### 3.1.1 Effect of $O_3$ dosage

Figure 1 shows that for SMX in ultrapure water with an initial concentration of 200 µg/L, approximately 99% of SMX can be decomposed when the $O_3$ concentration was higher than 1 mg/L. Thus, SMX can be quickly degraded during $O_3$ overdose. The removal rate of 10 mg/L SMX increased when the $O_3$ concentration was increased from 1 mg/L to 16 mg/L; this finding was related to the increased contact opportunities between $O_3$ and SMX.

#### 3.1.2 Effect of radical quencher

The removal rate of 200 µg/L SMX in the presence of 150 mmol/L *t*-BuOH was 98.6% when 10 mg/L $O_3$ was added; this rate was 0.6% lower than that in the absence of *t*-BuOH, indicating that most of the SMX was directly oxidized by $O_3$ at high concentrations of $O_3$ (Fig. 1(a)).

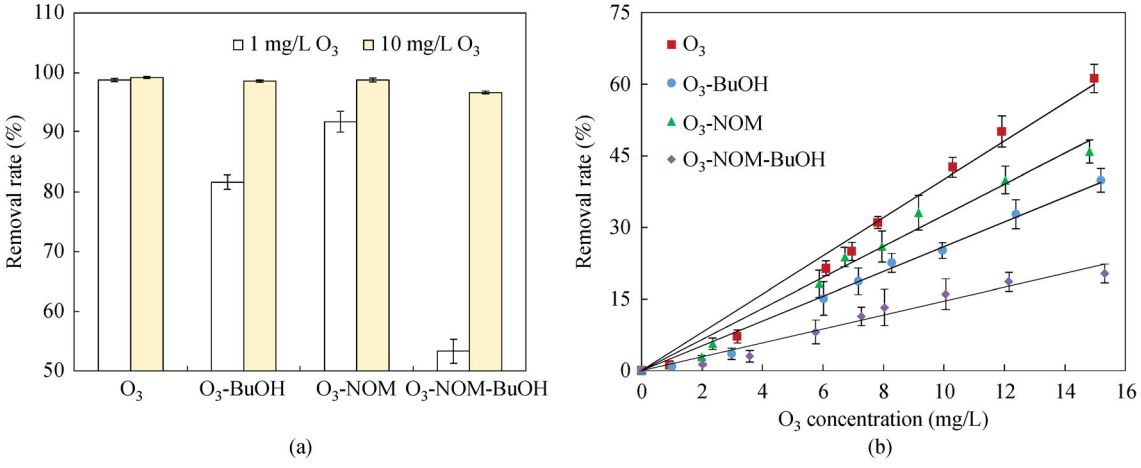


**Fig. 1** Influence of $O_3$ dosage on SMX removal rate: (a) 200 µg/L SMX; (b) 10 mg/L SMX (initial pH: 6.0; 0°C; "BuOH" means the addition of 150 mmol/L *t*-BuOH; "NOM" means the employment of the secondary effluent concentration with COD of 19 mg/L).

However, the removal rate reduced to 81.7% when 1 mg/L $O_3$ was employed. Thus, indirect oxidation also played an important role during the ozonation process. The results for the decomposition of 10 mg/L SMX (Fig. 1(b)) can also prove the combined effect of direct and indirect oxidation. The percentage of SMX degraded through direct oxidation was higher when excessive $O_3$ was supplied because the •OH generated from $O_3$ decomposition is unstable.

### 3.1.3 Effect of NOM

The removal rates of SMX in secondary effluent were considerably lower than those in ultrapure water, especially for the reaction system with low $O_3$ concentration; thus, NOM in water negatively affected the decomposition of micropollutants as NOM might consume $O_3$ or •OH during SMX ozonation (Lee and Lee, 2007; Liu et al., 2012), as was also observed during other advanced oxidation processes, such as photocatalysis (Ren et al., 2018) and persulfate oxidation (Qian et al., 2020). Moreover, the addition of *t*-BuOH in the secondary effluent quenched •OH, which can react with SMX, leading to the further reduction of the SMX removal rate (Fig. 1).

## 3.2 Degradation pathways of SMX by ozonation

### 3.2.1 SMX ozonation pathway

SMX can not be mineralized completely during ozonation. Ten kinds of intermediates with *m/z* of 269, 287, 173, 98, 78, 148, 152, 164, 166, and 180 were detected (Fig. S2). Figure 2 illustrates the proposed pathway for SMX ozonation. Figure 3 displays the evolution of the abundances of the abovementioned ozonation intermediates, which were calculated by dividing the peak areas of the intermediates by the initial peak area of SMX.

SMX ozonation involves four pathways: hydroxylation, hydrolysis, isoxazole-ring opening, and double-bond addition. P269, which is formed based on the attack to

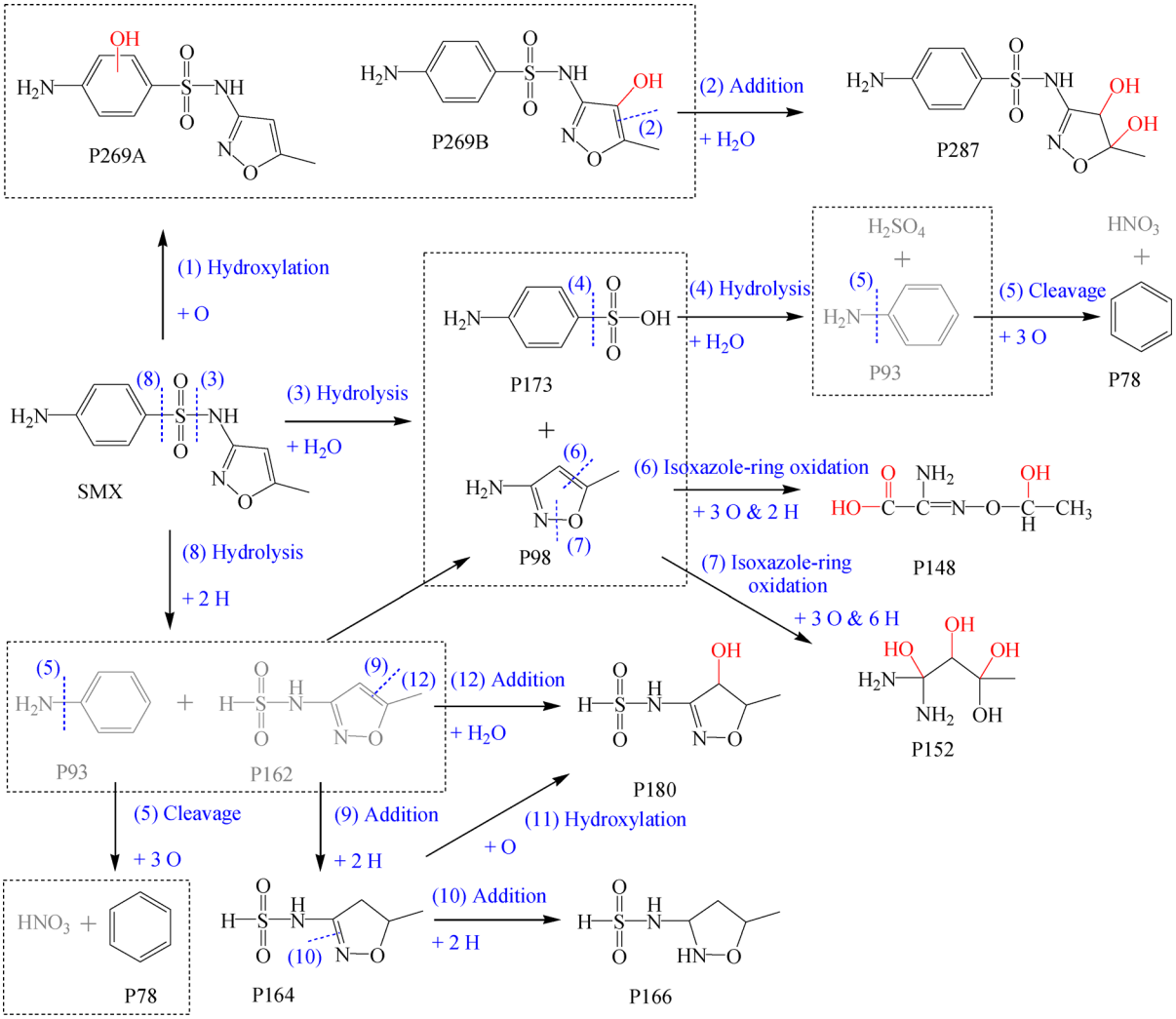


**Fig. 2** Ozonation pathways of SMX (initial SMX concentration: 10 mg/L; initial pH: 6.0; 20°C–22°C).

the benzene ring (P269A) (Du et al., 2018; Liu et al., 2020) or isoxazole-ring (P269B) by •OH (Zhang et al., 2017a; Li et al., 2019; Hai et al., 2020), is a hydroxylated product during ozonation (Guo et al., 2015). This product also forms during other advanced oxidation processes related to the generation of •OH (Niu et al., 2013; Yang et al., 2015). Intermediate P287, which is an oxidation product of $TiO_2$ photocatalysis (Zhang et al., 2017a) and photo-Fenton reaction (Trovó et al., 2009), was produced by the addition of $H_2O$ to the isoxazole-ring in P269B (Shahmahdi et al., 2020). The hydrolysis of the S–N bond led to generation of P173 (Lai et al., 2018; Shahmahdi et al., 2020) and P98 (Długosz et al., 2015; Li et al., 2019; Hai et al., 2020; Liu et al., 2020). Aniline, marked as P93, might have been generated by the loss of the sulfonic group from P173 during hydrolysis. However, no such product was detected because it was rapidly degraded to benzene (P78) and $HNO_3$. Moreover, P162 can be formed through hydrolysis. P148 and P152 were probably generated through isoxazole-ring opening, owing to the rapid reaction between $O_3$ and the organics containing electron-rich functional groups such as double-bonds (Westerhoff et al., 1999, Wang et al., 2019). Addition processes were also carried out on C = C or C = N double-bonds in P162, leading to the formation of P164, P166, and P180. Finally, the intermediate products can continually react with $O_3$ molecules or radicals to be completely decomposed into inorganic matters, such as $CO_2$, $H_2O$, $SO_4^{2-}$, and $NO_3^-$ (Augugliaro et al., 2012).

Figure 3(a) shows that most of the SMX was decomposed in less than 1 min. Figures 3(b) and 3(c) illustrate that the abundances of the hydroxylated products (P269 and P287) increased rapidly at first and then reduced a little, with the maximum abundances of 2.5% and 3.0%, respectively. The abundances of the hydrolyzed products, including P173, P98, and P78, exhibited similar trends with those of the hydroxylated products, except that the abundances declined remarkably (Figs. 3(d)–3(f), respectively). The maximum abundances of P173, P98, and P78 were 2.5%, 5.2%, and 0.2%, respectively. The value of P98 was considerably higher than that of P173 because the former may form from the hydrolysis of SMX and P162, whereas the latter can only be generated from SMX hydrolysis. The abundance for the isoxazole-ring opening product of P148, which was enhanced with the extension of processing period (8.4% at 10 min), was substantially higher than that of P152 (2.9% at 1.5 min) (Figs. 3(g) and 3 (h)). This result is attributed to the rapid reaction of $O_3$ with electron-rich functional groups, such as C = C double-bonds (Wang et al., 2019); for the non-selective •OH, the reaction between •OH and double-bonds was notably quicker (Westerhoff et al., 1999). Double-bond addition was also a major pathway for the decomposition of SMX. Figures 3(i)–3(k) show that in most cases, the abundances of addition products increased along with time, and the maximum abundances of these products were in the range of 2.5% to 53.9%. The above findings suggest that the lowest abundances of the hydrolyzed products were obtained because of their further degradation to isoxazole-ring opening and double-bond addition products. The small amounts of P269 and P287 imply that the hydroxylation process was not the principal route for SMX ozonation, which differed from the results observed with other advanced oxidation processes.

The toxicities of SMX and its ozonation intermediates were calculated by using the "Toxicity Estimation Software Tool" (V4.2.1 released by USEPA in 2016). The results shown in Table S1 indicate that no product with a stronger toxicity than SMX was formed, indicating that SMX and its intermediates lost their toxicity during ozonation.

### 3.2.2 Effect of radical quencher

*T*-BuOH was added to the SMX solution to distinguish the effects of direct and indirect ozonation. Figure 3 shows the abundances of intermediates during SMX ozonation in the presence of the radical quencher. After *t*-BuOH was added, the maximum abundances of P269 and P287 reduced by about 70%, indicating that the hydroxylated products were generated by the combined effect of direct and indirect oxidations, with •OH playing a major role. For hydrolyzed products, when •OH quencher was added, the maximum abundance of P173 reduced by approximately 50%. However, the abundance of P98 increased because of the strong inhibitory effect of the quencher on the formation of P78 (Figs. 3(d)–3(f)). Therefore, the generation of hydrolyzed products (P173 and P98) was attributed to the effect of direct and indirect oxidations, whereas the generation of P78 was related to indirect oxidation. No significant change was observed in the abundance of the isoxazole-ring opening product of P148 after the addition of *t*-BuOH (Fig. 3(g)). This finding can prove that $O_3$ attacks double bonds. However, the generation of P152 was abated because the cleavage of N–O mainly relied on the oxidation capacity of •OH (Fig. 3(h)). Figures 3(i)–3(k) show that during the double-bond addition process, the addition of •OH quencher showed minimal effect on the formation of these products. The inhibition effect on P164 was probably due to the suppression effect of *t*-BuOH on precursor P162.

In general, SMX was mainly degraded through hydrolysis, isoxazole-ring opening, and double-bond addition, and this result was attributed to the fast reaction between $O_3$ and electron-rich functional groups. Correspondingly, the generation of isoxazole-ring opening and double-bond addition products was not repressed after the •OH quencher was added. However, the formation of hydroxylated products was affected remarkably given its dependence on indirect oxidation. The hydrolyzed intermediates were produced by the combined effect of direct and indirect oxidations.

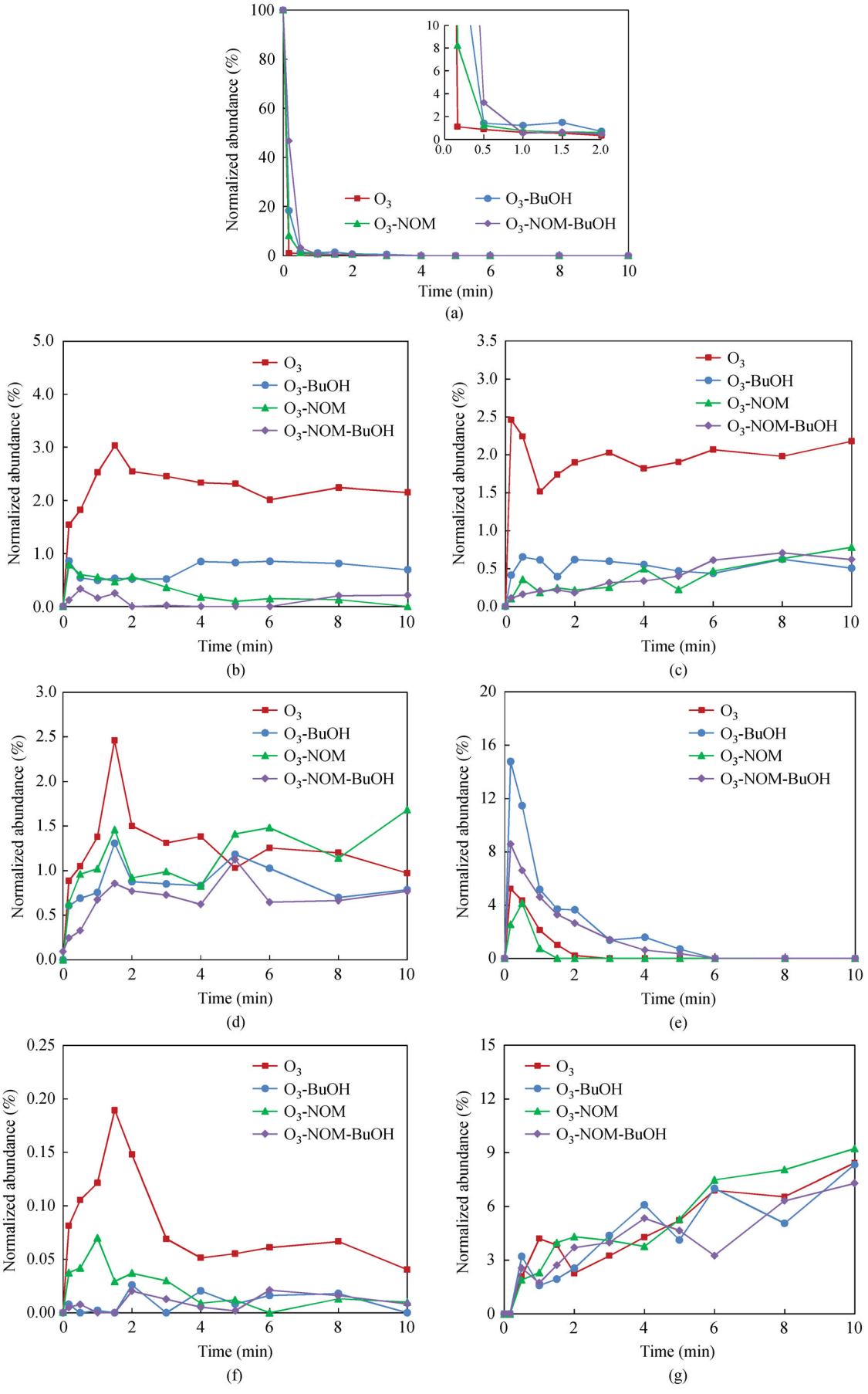
Normalized abundance (%)
Time (min)
O3
O3-BuOH
O3-NOM
O3-NOM-BuOH
(a)
(b)
(c)
(d)
(e)
(f)
(g)

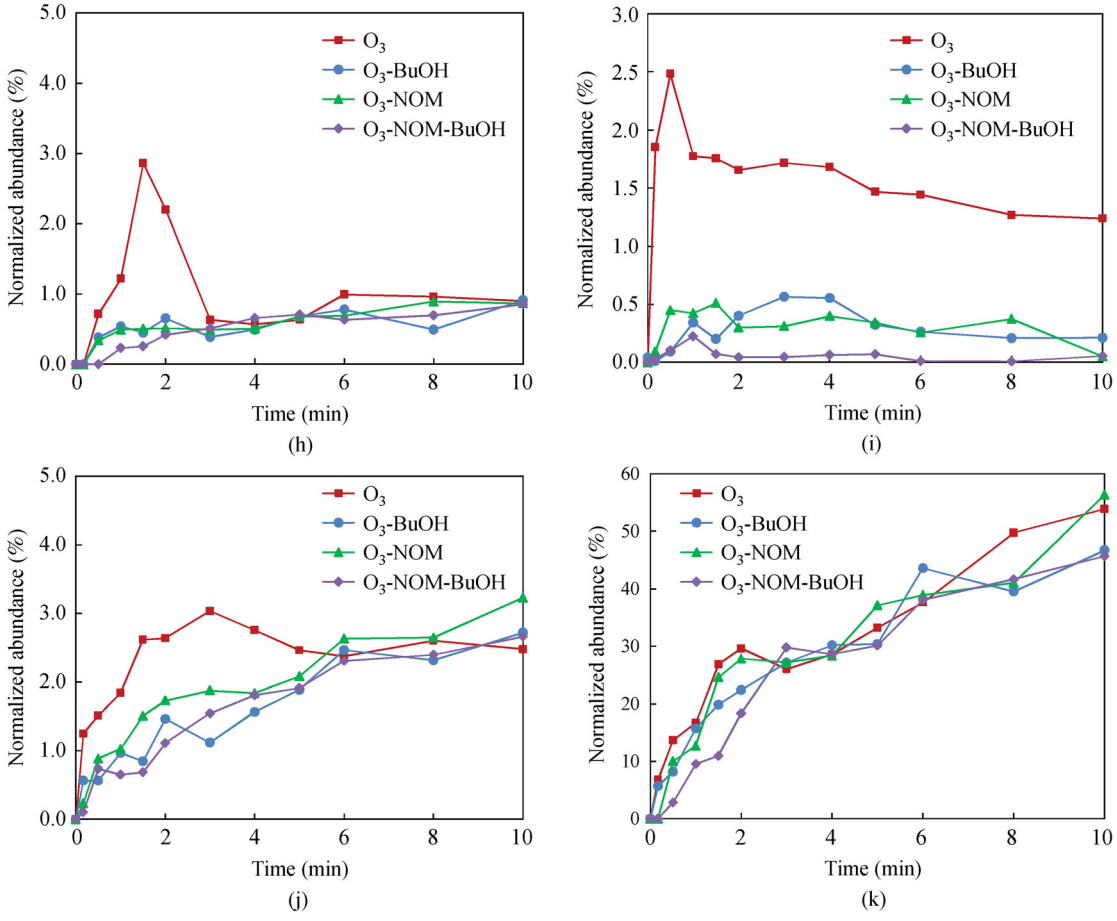


**Fig. 3** Evolution of intermediates from the ozonation of SMX: (a) SMX; (b) P269; (c) P287; (d) P173; (e) P98; (f) P78; (g) P148; (h) P152; (i) P164; (j) P166; (k) P180 (initial SMX concentration: 10 mg/L, initial pH: 6.0; 20°C–22°C; "BuOH" means the addition of 150 mmol/L *t*-BuOH; "NOM" means the employment of the secondary effluent concentration with COD of 37 mg/L).

### 3.2.3 Effect of NOM

The NOM in the secondary effluent can affect the decomposition of SMX and the formation of intermediates. The removal rate of SMX in the effluent at 10 s was lower than that in ultrapure water, and the value was further reduced after *t*-BuOH was added. The generation of P269, P287, P78, P152, and P164 was inhibited remarkably by NOM in the secondary effluent, with the maximum abundances reduced by as much as 74%, 85%, 63%, 70%, and 79%, respectively. Meanwhile, the maximum abundances of P173 and P166 were suppressed negligibly, and no significant effect was observed in the formation P98, P148, and P166. The results indicate that NOM in water can seriously influence the hydroxylation process, which depends on the indirect oxidation by •OH. The degradation pathways of hydrolysis and isoxazole-ring opening occurring on single-bonds were inhibited slightly after NOM were added. The major SMX degradation pathways of isoxazole-ring opening (on double bond) and double-bond addition were not visibly affected by the NOM in the effluent because excessive $O_3$ molecules are more likely to attack electron-rich functional groups such as double-bonds (Westerhoff et al., 1999; Wang et al., 2019).

The addition of *t*-BuOH in the effluent led to the further reduction of the maximum abundances of hydroxylated and hydrolyzed products, including P269, P173, and P78; this result proves that NOM can react not only with •OH, but also $O_3$ molecules (Lee and Lee, 2007). However, the abundances of intermediates that were mainly produced through direct oxidation (isoxazole-ring opening and double-bond addition) were not affected remarkably. Thus, the NOM in the secondary effluent mainly affected the degradation of micropollutants by consuming •OH.

## 3.3 Ozonation of DOM in secondary effluent

### 3.3.1 Changes in the organic component content

Figures 4 and S3–S5 illustrate the 3DEEMFS maps of the NOM in the effluent during ozonation. The map was divided into five regions: R-I, tyrosine-based aromatic

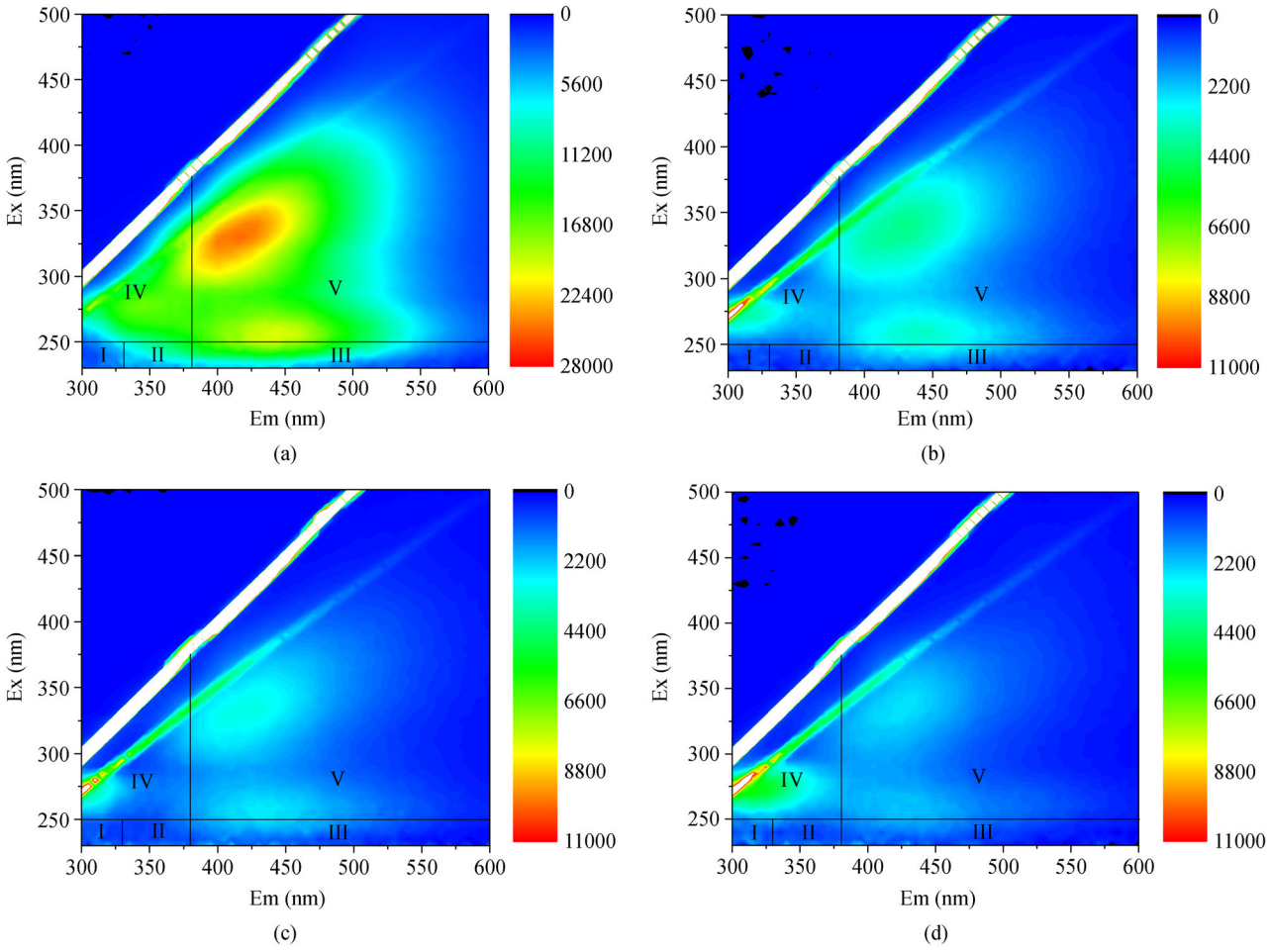


**Fig. 4** 3DEEMFS maps of NOM in secondary effluent during ozonation: (a) 0, (b) 2, (c) 5, and (d) 10 min (initial SMX concentration: 200 μg/L; initial pH: 6.0; COD: 37 mg/L; 20°C–22°C).

proteins with $\lambda_{ex/em}$ of 230–250/280–330 nm; R-II, tryptophan-based aromatic proteins with $\lambda_{ex/em}$ of 230–250/330–380 nm; R-III, fulvic acid-like substances with $\lambda_{ex/em}$ of 230–275/380–550 nm; R-IV, soluble microbial byproducts consisting of tyrosine, phenylcyclic proteins, high-excitation tyrosine, and high-excitation tryptophan, with $\lambda_{ex/em}$ of 250–300/280–380 nm; R-V, humic acid-like substances with $\lambda_{ex/em}$ of 275–345/380–550 nm (Chen et al., 2003). Figures. S6 and 5 show the standard integral volumes of NOM.

Figure 5(a) shows that all of the abovementioned substances were found in the secondary effluent, and their standard integral volumes decreased during ozonation. R-II, R-III, and R-V were easily degraded because of their high degree of unsaturation.

Three main fluorescence peaks were observed in the 3DEEMFS maps (Figs. S7 and 6): Peak B, protein-like substances produced by microbial metabolism with $\lambda_{Ex/Em}$ of 275–285/310–320 nm; Peak M, fulvic-like substances with $\lambda_{Ex/Em}$ of 330–340/410–420 nm; Peak A, ultraviolet A (UVA) humic-like substances with $\lambda_{Ex/Em}$ of 245–255/410–420 nm (Jiao et al., 2018). The removal efficiencies of humic-like and fulvic-like substances were notably higher than that of protein-like substances.

The changes in the regions in 3DEEMFS maps and the fluorescence peaks of the components in the secondary effluent were not influenced by the addition of 200 μg/L SMX because the SMX concentration was notably lower than that of NOM (Figs. 5(a), 5(c), 6(a), and 6(c)).

### 3.3.2 Effect of radical quencher

After *t*-BuOH was added, the removal efficiencies in all the regions reduced, showing that •OH played an important role during ozonation. The inhibitory effect of the quencher on the components followed the sequence of UVA humic-like substances (Peak A)>fluvic-like substances (Peak M)>protein-like substances (Peak B). The NOM with a short emission wavelength fluorescence signal (Peak A) were related to simple structural components with low degree of aromatic condensation (Senesi et al., 2003); components with longer emission

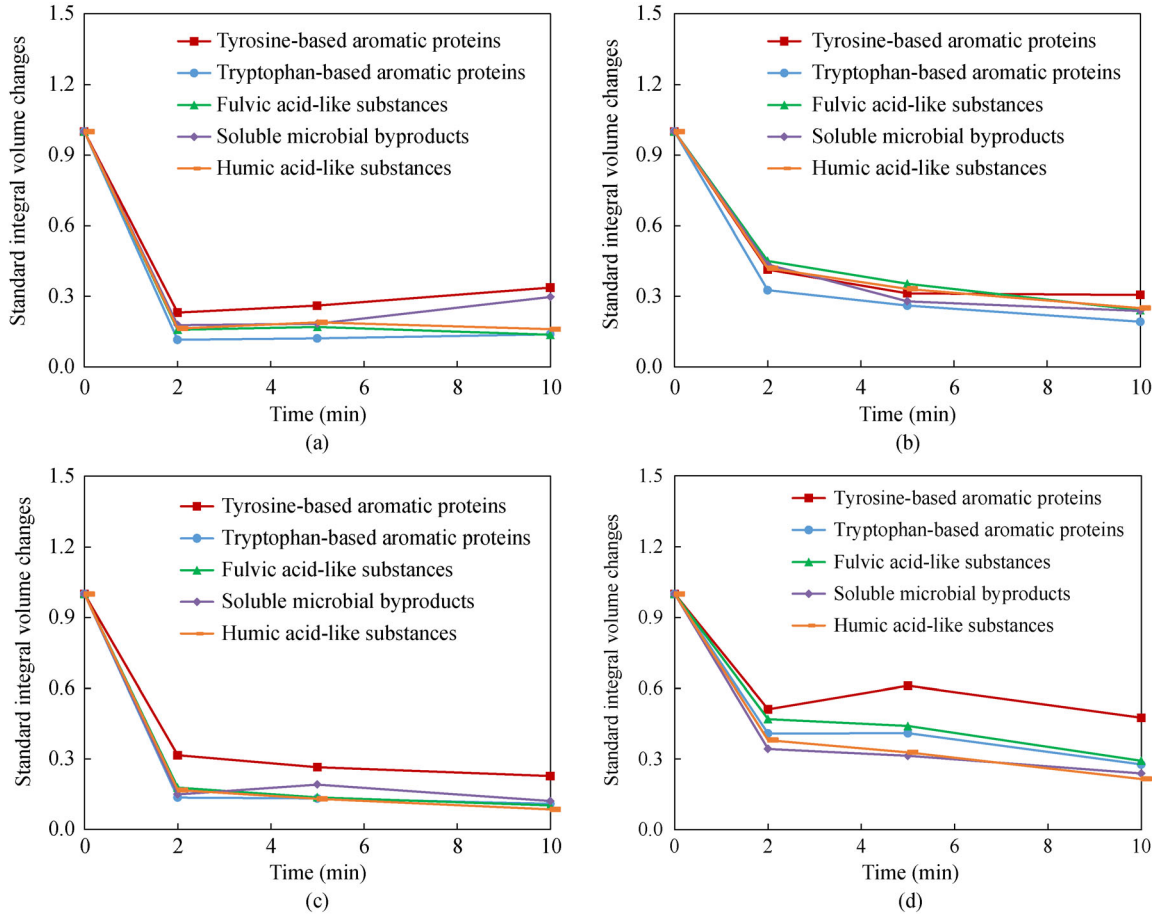


**Fig. 5** Changes in the standard integral volume of NOM in secondary effluent during ozonation: (a) in the presence of 200 μg/L SMX; (b) in the presence of 200 μg/L SMX and 150 mmol/L *t*-BuOH; (c) in the absence of 200 μg/L SMX; (d) in the presence 150 mmol/L *t*-BuOH (initial pH: 6.0, COD: 37 mg/L; 20°C–22°C).

wavelengths, including Peak B and Peak M, represent larger molecular weights, more conjugated components, and more complex structures (Milori et al., 2002); the component of Peak M, which contained a large amount of aromatic carbon, was representative of several refractory organics (McKnight et al., 1994). Therefore, the suppression effect of *t*-BuOH was related to the aromaticity of the components, and the degradation of NOM with a high degree of aromatic condensation was abated given that the direct oxidation by $O_3$ molecule occurred in the organic-rich electronic functional groups (Wang et al., 2019). Similar with those in the absence of $^{\bullet}OH$ quencher, 200 μg/L SMX in the effluent had no significant effect on the fluorescence peaks of the components (Figs. 6(a) and 6(c)).

## 4 Conclusions

In the present work, the ozonation mechanism of SMX was revealed, and the influencing mechanism of NOM on SMX ozonation pathways was explored. In general, SMX was mainly degraded through hydrolysis, isoxazole-ring opening, and double-bond addition during ozonation, but hydroxylation, as often reported in previous studies on the advanced oxidation of SMX, was not the principal route. Correspondingly, the generation of isoxazole-ring opening and double-bond addition products was related to direct oxidation. However, the formation of hydroxylated products depended on indirect oxidation, whereas hydrolyzed intermediates were produced by the combined effects of direct and indirect oxidations. The decomposition pathways of SMX were affected by NOM in the secondary effluent. The hydroxylation process, which depends on the indirect oxidation, was seriously influenced by NOM, and the major SMX degradation pathways of hydrolysis, isoxazole-ring opening, and double-bond addition were barely affected. The NOM mainly affected the degradation of micro-pollutants by consuming $^{\bullet}OH$ rather than $O_3$ molecules.

The NOM in water can be simultaneously degraded during ozonation. Three main fluorescence peaks representing protein-, fulvic-, and UVA humic-like substances

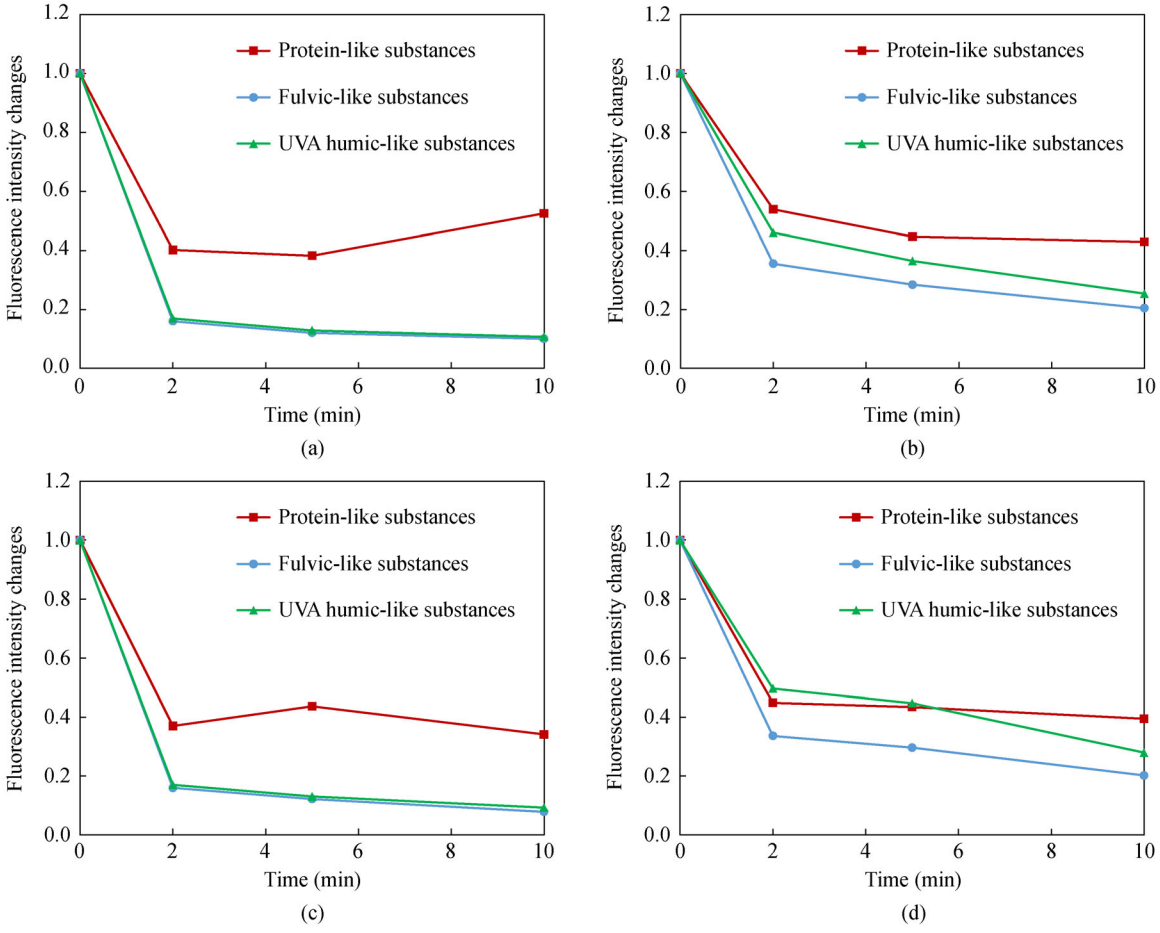


**Fig. 6** Changes in the fluorescence intensity of the main components in secondary effluent during ozonation: (a) in the presence of 200 μg/L SMX; (b) in the presence of 200 μg/L SMX and 150 mmol/L *t*-BuOH; (c) in the absence of 200 μg/L SMX; (d) in the presence 150 mmol/L *t*-BuOH (initial pH: 6.0; COD: 37 mg/L; 20°C–22°C).

were found in the secondary effluent. The removal of all components was abated by the radical quencher, and the inhibitory effect on the components followed the sequence: UVA humic-like substances>fluvic-like substances>protein-like substances. This condition was related to the aromaticity of the components. The removal rates of these components were unaffected by the addition of 200 μg/L SMX because of the low SMX concentration.

**Acknowledgements** This work was supported by the National Key Research and Development Project (No. 2019YFD1100204). The experimental supporting by National Environmental and Energy Base for International Science & Technology Cooperation was greatly appreciated.

**Electronic Supplementary Material** Supplementary material is available in the online version of this article at https://doi.org/10.1007/s11783-020-1367-1 and is accessible for authorized users.

## References

Augugliaro V, Bellardita M, Loddo V, Palmisano G, Palmisano L, Yurdakal S (2012). Overview on oxidation mechanisms of organic compounds by $TiO_2$ in heterogeneous photocatalysis. Journal of Photochemistry and Photobiology C, Photochemistry Reviews, 13 (3): 224–245

Bader H, Hoigné J (1981). Determination of ozone in water by the indigo method. Water Research, 15(4): 449–456

Buxton G V, Greenstock C L, Helman W P, Ross A B (1988). Critical review of rate constants for reactions of hydrated electrons, hydrogen atoms and hydroxyl radicals (·OH/·O⁻) in aqueous solution. Journal of Physical and Chemical Reference Data, 17(2): 513

Chen S, Blaney L, Chen P, Deng S, Hopanna M, Bao Y, Yu G (2019). Ozonation of the 5-fluorouracil anticancer drug and its prodrug capecitabine: Reaction kinetics, oxidation mechanisms, and residual toxicity. Frontiers of Environmental Science & Engineering, 13(4): 59

Chen W, Westerhoff P, Leenheer J A, Booksh K (2003). Fluorescence excitation-emission matrix regional integration to quantify spectra for dissolved organic matter. Environmental Science & Technology, 37 (24): 5701–5710

Coble P G (1996). Characterization of marine and terrestrial DOM in seawater using excitation-emission matrix spectroscopy. Marine Chemistry, 51(4): 325–346

Długosz M, Zmudzki P, Kwiecien A, Szczubialka K, Krzek J,

Nowakowska M (2015). Photocatalytic degradation of sulfamethoxazole in aqueous solution using a floating $TiO_2$-expanded perlite photocatalyst. Journal of Hazardous Materials, 298: 146–153

Du J, Guo W, Wang H, Yin R, Zheng H, Feng X, Che D, Ren N (2018). Hydroxyl radical dominated degradation of aquatic sulfamethoxazole by $Fe^0$/bisulfite/$O_2$: Kinetics, mechanisms, and pathways. Water Research, 138: 323–332

Gómez-Ramos M del MMezcua M, Aguera A, Fernandez-Alba A R, Gonzalo S, Rodriguez A, Rosal R (2011). Chemical and toxicological evolution of the antibiotic sulfamethoxazole under ozone treatment in water solution. Journal of Hazardous Materials, 192(1): 18–25

Graça C A L, Lima R B, Pereira M F R, Silva A M T, Ferreira A (2020). Intensification of the ozone-water mass transfer in an oscillatory flow reactor with innovative design of periodic constrictions: Optimization and application in ozonation water treatment. Chemical Engineering Journal, 389: 124412

Guo W Q, Yin R L, Zhou X J, Du J S, Cao H O, Yang S S, Ren N Q (2015). Sulfamethoxazole degradation by ultrasound/ozone oxidation process in water: Kinetics, mechanisms, and pathways. Ultrasonics Sonochemistry, 22: 182–187

Hai H, Xing X, Li S, Xia S, Xia J (2020). Electrochemical oxidation of sulfamethoxazole in BDD anode system: Degradation kinetics, mechanisms and toxicity evaluation. Science of the Total Environment, 738: 139909

Ho L, Newcombe G, Croué J P (2002). Influence of the character of NOM on the ozonation of MIB and geosmin. Water Research, 36(3): 511–518

Ioannidi A, Oulego P, Collado S, Petala A, Arniella V, Frontistis Z, Angelopoulos G N, Diaz M, Mantzavinos D (2020). Persulfate activation by modified red mud for the oxidation of antibiotic sulfamethoxazole in water. Journal of Environmental Management, 270: 110820

Jiao Y, Zhao Y, Chen Y, Wu G, Liu W, Tian X, Zheng Y (2018). Characterizing the interaction of sulfamethazine and macrophytes-derived dissolved organic matter by fluorescence spectroscopy. Environmental Science & Technology, 41(3): 8–14

Khan A H, Khan N A, Ahmed S, Dhingra A, Singh C P, Khan S U, Mohammadi A A, Changani F, Yousefi M, Alam S, Vambol S, Vambol V, Khursheed A, Ali I (2020a). Application of advanced oxidation processes followed by different treatment technologies for hospital wastewater treatment. Journal of Cleaner Production, 269: 122411

Khan N A, Ahmed S, Farooqi I H, Ali I, Vambol V, Changani F, Yousefi M, Vambol S, Khan S U, Khan A H (2020b). Occurrence, sources and conventional treatment techniques for various antibiotics present in hospital wastewaters: A critical review. Trends in Analytical Chemistry, 129: 115921

Khan N A, Khan S U, Ahmed S, Farooqi I H, Yousefi M, Mohammadi A A, Changani F (2020c). Recent trends in disposal and treatment technologies of emerging-pollutants-A critical review. Trends in Analytical Chemistry, 122: 115744

Kong S, Zhao Y G, Guo L, Gao M, Jin C, She Z (2020). Transcriptomics of Planococcus kocurii O516 reveals the degrading metabolism of sulfamethoxazole in marine aquaculture wastewater. Environmental Pollution, 265: 114939

Lai L, Yan J, Li J, Lai B (2018). Co/$Al_2O_3$-EPM as peroxymonosulfate activator for sulfamethoxazole removal: Performance, biotoxicity, degradation pathways and mechanism. Chemical Engineering Journal, 343: 676–688

Lee C Y, Lee Y (2007). Impact of water quality on the formation of bromate and formaldehyde during water ozonation. Korean Journal of Environmental Health, 33(5): 441–450

Li H, Li T, He S, Zhou J, Wang T, Zhu L (2020a). Efficient degradation of antibiotics by non-thermal discharge plasma: Highlight the impacts of molecular structures and degradation pathways. Chemical Engineering Journal, 395: 125091

Li S, Hu J (2018). Transformation products formation of ciprofloxacin in UVA/LED and UVA/LED/$TiO_2$ systems: Impact of natural organic matter characteristics. Water Research, 132: 320–330

Li Y, Li J, Pan Y, Xiong Z, Yao G, Xie R, Lai B (2020b). Peroxymonosulfate activation on $FeCo_2S_4$ modified g-$C_3N_4$ ($FeCo_2S_4$-CN): Mechanism of singlet oxygen evolution for non-radical efficient degradation of sulfamethoxazole. Chemical Engineering Journal, 384: 123361

Li Y, Zhao X, Yan Y, Yan J, Pan Y, Zhang Y, Lai B (2019). Enhanced sulfamethoxazole degradation by peroxymonosulfate activation with sulfide-modified microscale zero-valent iron (S-m$Fe^0$): Performance, mechanisms, and the role of sulfur species. Chemical Engineering Journal, 376: 121302

Liu F, Zhou H, Pan Z, Liu Y, Yao G, Guo Y, Lai B (2020). Degradation of sulfamethoxazole by cobalt-nickel powder composite catalyst coupled with peroxymonosulfate: Performance, degradation pathways and mechanistic consideration. Journal of Hazardous Materials, 400: 123322

Liu X, Garoma T, Chen Z, Wang L, Wu Y (2012). SMX degradation by ozonation and UV radiation: a kinetic study. Chemosphere, 87(10): 1134–1140

Mao Y, Dong H, Liu S, Zhang L, Qiang Z (2020). Accelerated oxidation of iopamidol by ozone/peroxymonosulfate ($O_3$/PMS) process: Kinetics, mechanism, and simultaneous reduction of iodinated disinfection by-product formation potential. Water Research, 173: 115615

McKnight D M, Andrews E D, Spaulding S A, Aiken G R (1994). Aquatic fulvic acids in algal-rich antarctic ponds. Limnology and Oceanography, 39(8): 1972–1979

Milh H, Schoenaers B, Stesmans A, Cabooter D, Dewil R (2020). Degradation of sulfamethoxazole by heat-activated persulfate oxidation: Elucidation of the degradation mechanism and influence of process parameters. Chemical Engineering Journal, 379: 122234

Milori D M B P, Martin-Neto L, Bayer C, Mielniczuk J, Bagnato V S (2002). Humification degree of soil humic acids determined by fluorescence spectroscopy. Soil Science, 167(11): 739–749

Ninwiwek N, Hongsawat P, Punyapalakul P, Prarat P (2019). Removal of the antibiotic sulfamethoxazole from environmental water by mesoporous silica-magnetic graphene oxide nanocomposite technology: Adsorption characteristics, coadsorption and uptake mechanism. Colloids and Surfaces. A, Physicochemical and Engineering Aspects, 580: 123716

Niu J, Zhang L, Li Y, Zhao J, Lv S, Xiao K (2013). Effects of environmental factors on sulfamethoxazole photodegradation under simulated sunlight irradiation: Kinetics and mechanism. Journal of Environmental Sciences-China, 25(6): 1098–1106

Qian Y, Liu X, Li K, Gao P, Chen J, Liu Z, Zhou X, Zhang Y, Chen H, Li X, Xue G (2020). Enhanced degradation of cephalosporin antibiotics by matrix components during thermally activated persulfate oxidation process. Chemical Engineering Journal, 384: 123332

Ren M, Drosos M, Frimmel F H (2018). Inhibitory effect of NOM in photocatalysis process: Explanation and resolution. Chemical Engineering Journal, 334: 968–975

Senesi N, D'orazio V, Ricca G (2003). Humic acids in the first generation of EUROSOILS. Geoderma, 116(3–4): 325–344

Shahmahdi N, Dehghanzadeh R, Aslani H, Bakht Shokouhi S (2020). Performance evaluation of waste iron shavings ($Fe^0$) for catalytic ozonation in removal of sulfamethoxazole from municipal wastewater treatment plant effluent in a batch mode pilot plant. Chemical Engineering Journal, 383: 123093

Trovó A G, Nogueira R F, Aguera A, Fernandez-Alba A R, Sirtori C, Malato S (2009). Degradation of sulfamethoxazole in water by solar photo-Fenton. Chemical and toxicological evaluation. Water Research, 43(16): 3922–3931

Wang H, Mustafa M, Yu G, Ostman M, Cheng Y, Wang Y, Tysklind M (2019). Oxidation of emerging biocides and antibiotics in wastewater by ozonation and the electro-peroxone process. Chemosphere, 235: 575–585

Wang J, Chu L (2016). Irradiation treatment of pharmaceutical and personal care products (PPCPs) in water and wastewater: An overview. Radiation Physics and Chemistry, 125: 56–64

Wang J, Zhuan R (2020). Degradation of antibiotics by advanced oxidation processes: An overview. Science of the Total Environment, 701: 135023 doi:10.1016/j.scitotenv.2019.135023

Westerhoff P, Aiken G, Amy G, Debroux J (1999). Relationships between the structure of natural organic matter and its reactivity towards molecular ozone and hydroxyl radicals. Water Research, 33 (10): 2265–2276

Willach S, Lutze H V, Eckey K, Loppenberg K, Luling M, Terhalle J, Wolbert J B, Jochmann M A, Karst U, Schmidt T C (2017). Degradation of sulfamethoxazole using ozone and chlorine dioxide-Compound-specific stable isotope analysis, transformation product analysis and mechanistic aspects. Water Research, 122: 280–289

Xiao K, Yu J, Wang S, Du J, Tan J, Xue K, Wang Y, Huang X (2020). Relationship between fluorescence excitation-emission matrix properties and the relative degree of DOM hydrophobicity in wastewater treatment effluents. Chemosphere, 254: 126830

Yang C C, Huang C L, Cheng T C, Lai H T (2015). Inhibitory effect of salinity on the photocatalytic degradation of three sulfonamide antibiotics. International Biodeterioration & Biodegradation, 102: 116–125

Ye B, Chen Z, Li X, Liu J, Wu Q, Yang C, Hu H, Wang R (2019). Inhibition of bromate formation by reduced graphene oxide supported cerium dioxide during ozonation of bromide-containing water. Frontiers of Environmental Science & Engineering, 13 (6): 86

Yu H, Qu F, Zhang X, Shao S, Rong H, Liang H, Bai L, Ma J (2019). Development of correlation spectroscopy (COS) method for analyzing fluorescence excitation emission matrix (EEM): A case study of effluent organic matter (EfOM) ozonation. Chemosphere, 228: 35–43

Yuan R, Zhu Y, Zhou B, Hu J (2019). Photocatalytic oxidation of sulfamethoxazole in the presence of $TiO_2$: Effect of matrix in aqueous solution on decomposition mechanisms. Chemical Engineering Journal, 359: 1527–1536

Zhang H, Wang Z, Li R, Guo J, Li Y, Zhu J, Xie X (2017a). $TiO_2$ supported on reed straw biochar as an adsorptive and photocatalytic composite for the efficient degradation of sulfamethoxazole in aqueous matrices. Chemosphere, 185: 351–360

Zhang S, Yu G, Chen J, Zhao Q, Zhang X, Wang B, Huang J, Deng S, Wang Y (2017b). Elucidating ozonation mechanisms of organic micropollutants based on DFT calculations: Taking sulfamethoxazole as a case. Environmental Pollution, 220: 971–980

Zhang T, Tao Y Z, Yang H W, Chen Z, Wang X M, Xie Y F (2020). Study on the removal of aesthetic indicators by ozone during advanced treatment of water reuse. Journal of Water Process Engineering, 36: 101381

Zhao X, Wu Y, Zhang X, Tong X, Yu T, Wang Y, Ikuno N, Ishii K, Hu H (2019). Ozonation as an efficient pretreatment method to alleviate reverse osmosis membrane fouling caused by complexes of humic acid and calcium ion. Frontiers of Environmental Science & Engineering, 13(4): 55

Zhou J, Wang J J, Baudon A, Chow A T (2013). Improved fluorescence excitation-emission matrix regional integration to quantify spectra for fluorescent dissolved organic matter. Journal of Environmental Quality, 42(3): 925–930